3D bioprinting mesenchymal stem cell-laden construct with core–shell nanospheres for cartilage tissue engineering

IOP Publishing Nanotechnology
Nanotechnology 29 (2018) 185101 (10pp) https://doi.org/10.1088/1361-6528/aaafa1

3D bioprinting mesenchymal stem cell-laden construct with core–shell nanospheres for cartilage tissue engineering

Wei Zhu[1], Haitao Cui[1], Benchaa Boualam[2], Fahed Masood[2], Erin Flynn[3], Raj D Rao[3], Zhi-Yong Zhang[4] and Lijie Grace Zhang[1,5,6]

[1] Department of Mechanical and Aerospace Engineering, The George Washington University, Washington DC 20052, United States of America
[2] University of Maryland-College Park, United States of America
[3] Department of Orthopaedic Surgery, The George Washington University, Washington DC 20052, United States of America
[4] Translational Research Centre of Regenerative Medicine and 3D Printing Technologies of Guangzhou Medical University, The Third Affiliated Hospital of Guangzhou Medical University, Guangzhou City, Guangdong Province, 510150, People's Republic of China
[5] Department of Biomedical Engineering, The George Washington University, Washington DC 20052, United States of America
[6] Department of Medicine, The George Washington University, Washington DC 20052, United States of America

E-mail: lgzhang@gwu.edu

Received 6 November 2017, revised 9 February 2018
Accepted for publication 15 February 2018
Published 8 March 2018

Abstract

Cartilage tissue is prone to degradation and has little capacity for self-healing due to its avascularity. Tissue engineering, which provides artificial scaffolds to repair injured tissues, is a novel and promising strategy for cartilage repair. 3D bioprinting offers even greater potential for repairing degenerative tissue by simultaneously integrating living cells, biomaterials, and biological cues to provide a customized scaffold. With regard to cell selection, mesenchymal stem cells (MSCs) hold great capacity for differentiating into a variety of cell types, including chondrocytes, and could therefore be utilized as a cartilage cell source in 3D bioprinting. In the present study, we utilize a tabletop stereolithography-based 3D bioprinter for a novel cell-laden cartilage tissue construct fabrication. Printable resin is composed of 10% gelatin methacrylate (GelMA) base, various concentrations of polyethylene glycol diacrylate (PEGDA), biocompatible photoinitiator, and transforming growth factor beta 1 (TGF-β1) embedded nanospheres fabricated via a core–shell electrospraying technique. We find that the addition of PEGDA into GelMA hydrogel greatly improves the printing resolution. Compressive testing shows that modulus of the bioprinted scaffolds proportionally increases with the concentrations of PEGDA, while swelling ratio decreases with the increase of PEGDA concentration. Confocal microscopy images illustrate that the cells and nanospheres are evenly distributed throughout the entire bioprinted construct. Cells grown on 5%/10% (PEGDA/GelMA) hydrogel present the highest cell viability and proliferation rate. The TGF-β1 embedded in nanospheres can keep a sustained release up to 21 d and improve chondrogenic differentiation of encapsulated MSCs. The cell-laden bioprinted cartilage constructs with TGF-β1-containing nanospheres is a promising strategy for cartilage regeneration.

Keywords: 3D bioprinting, nanosphere, mesenchymal stem cell, cartilage tissue engineering

(Some figures may appear in colour only in the online journal)

1. Introduction

Articular cartilage is precisely organized to facilitate smooth motion between diarthrodial joints. However, it is prone to degradation secondary to trauma, disease, or aging. Due to its avascular nature, damaged articular cartilage is unable to access nutrients or circulating progenitor cells, resulting in extremely limited intrinsic regenerative capacity [1]. Surgical intervention is required for most severe cartilage injures. Tissue engineering, which manipulates cells, scaffolds, and stimuli, promotes repair and recovery of injured cartilage by providing an artificial functional construct. Upon implantation, the artificial construct integrates with native tissues and recovers lost function. In order to produce 3D tissue constructs that mimic native tissues' structure, the cells and extracellular matrix (ECM) must be patterned in a precise geometric formation [2]. With respect to cartilage regeneration, where mesenchymal stem cells (MSC) are one of the main cell lines used in cartilage healing by tissue engineering strategy, studies have demonstrated that the microstructure of cell culture matrix influences both MSC proliferation and chondrogenic differentiation [3]. Taking these developments into consideration, the emerging 3D printing is superior to other strategies of tissue construct fabrication.

3D printing is primarily designed to produce acellular 3D scaffolds or sacrificial molds, with cells seeded onto the scaffolds postprinting [4]. Recent advances in material science and cell technology have paved the way for 3D printing to simultaneously deposit living cells and biological materials to build 'living' 3D constructs, a process known as 3D bioprinting [5]. In addition to engineering tissue constructs, 3D bioprinting has attempted to develop cell-based sensors and disease models [6, 7]. The challenge in 3D bioprinting is the selection of bioink, which must not only generate a 'cell-friendly condition', but also meet the requirements needed for good printability [8]. The choice of bioink is also limited by bioprinting techniques. Three mainstream bioprinting technologies: inkjet, microextrusion, and laser-assisted printing, have different requirements regarding the bioink properties [5, 9–11]. Regardless of bioprinting technology, materials currently used in the field of tissue engineering are primarily divided into either natural based polymers or synthetic molecules [5]. Natural polymers are biocompatible and bioactive with similarity to human ECM, but their mechanical properties are usually less than ideal. Compared to natural polymers, synthetic polymers are more easily tailored with specific physical properties. 3D bioprinting requires the bioink to be biocompatible for long-term transplantation, have suitable crosslinking ability to allow for the building of a 3D construct, and maintain initial mechanical properties without collapsing.

Human tissues are surrounded by natural ECM, which contains a wide range of bioactive signals that influence cell fate. Growth factors are usually introduced into tissue engineering in effort to regulate cell functions in both a spatial and temporal manner. Without protection, however, growth factors are susceptible to degradation and are eliminated rapidly even with high-dose administration [12]. A delivery system with encapsulation of growth factors has demonstrated considerable promise in addressing these issues. This delivery system can act as a depot for retention of growth factors in high concentration and protective environment for carrying growth factors to treatment sites and keeping sustained release. Polymer-based delivery systems have enjoyed a privileged status due to their multiple advantages, including their lack of potential immunogenicity and the ease of modulating their properties such as biodegradability, biocompatibility, and reproducibility [13, 14]. Poly(lactic-co-glycolic acid) (PLGA) is one of the most attractive polymers for development of a delivery vehicle because of its excellent biocompatibility and physiochemical properties [15]. PLGA carriers are hydrolytically degraded over time both *in vitro* and *in vivo*, and the release kinetics of PLGA carriers can be easily fine-tuned by adjusting the ratio of poly(lactic acid) to poly(glycolic acid) [16].

In the present study, we applied a stereolithography-based 3D bioprinter to create a cartilage construct by using bioink consisting of MSCs, modified gelatin, and PEGDA. In addition, a PLGA-based growth factor carrier system was developed via an electrospraying method. Transforming growth factor beta 1 (TGF-β1) was encapsulated and delivered with the 3D bioprinted construct. The cell viability, growth and chondrogenic differentiation were investigated in an effort to develop an optimal 3D bioprinted construct for cartilage regeneration.

2. Materials and methods

2.1. Bioink preparation

Gelatin (Type A, Sigma-Aldrich) was modified by methacrylic anhydride to render the photo-curable capacity with an established approach [17, 18]. Briefly, 10% gelatin was dissolved in phosphate buffer saline (PBS) with stirring at 50 °C until a clear solution was observed. Methacrylic anhydride was then added at 5% of the entire clear solution with a rate of 0.5 ml min^{-1}. The mixture was allowed to react for 1 h at 50 °C followed by dialyzing through a cellulose membrane bag (14 kDa typical molecular weight cut-off) in deionized water. After 4 d of dialysis, the mixture was frozen and lyophilized to produce white porous gelatin methacrylate (GelMA).

TGF-β1-embedded core–shell nanospheres were synthesized via co-axial electrospraying method as described in our previous study [19]. TGF-β1 was added into 1% bovine serum albumin (BSA)/PBS at a concentration of 1000 ng ml^{-1} as core solution. The shell solution was composed of 2.5% PLGA (50:50) in acetone. The co-axial needle has 20 G outer and 26 G inner sizes. Electrospraying was performed at 7 kV voltage and 2.5 ml h^{-1} flow rate. Electrosprayed nanospheres were stirred a half hour to remove the organic solvent and then lyophilized. Morphology of nanospheres was visualized by transmission electron microscope (Zeiss NVision 40 FIB). The bioink was prepared by mixing GelMA, polyethylene glycol diacrylate (PEGDA, Mn = 700), biocompatible photoinitiator (2-Hydroxy-4′-(2-

hydroxyethoxy)-2-methylpropiophenone, Sigma-Aldrich), and TGF-β1-embedded nanospheres.

2.2. Hydrogels characterization

10% GelMA base was blended with PEGDA at a concentration range of 5%–20% at 60 °C and solidified by UV (355 nm) for 45 s to generate hydrogel samples for characterization. The compressive mechanical properties of each composition were measured by an MTS criterion universal testing system equipped with a 100 N load cell (MTS Corporation, US). The crosshead speed was set as 2 mm min^{-1}. The experiment was performed under ambient conditions. Compressive modulus was calculated at 40% strain based on the strain–stress curves. The equilibrium degree of swelling for various hydrogels was obtained to estimate structural parameters. In brief, hydrogels were dried at 60 °C in the oven and the dry mass (M_D) was measured. The dried samples were then immersed in PBS and incubated at 37 °C until swelling equilibrium. The swelling mass was measured as M_S. The equilibrium swelling ratio was calculated using equation of $(M_S - M_D)/M_D$. In addition, the printing resolution for each composition was evaluated by measuring the line width after printing the precursor solutions using our 3D bioprinter introduced below.

2.3. Cell culture

Human bone marrow MSCs were maintained in a humidified atmosphere with 5% CO_2 at 37 °C. The cells were harvested from healthy consenting donors in the Texas A&M Health Science Center, Institute for Regenerative Medicine. For expansion, cell culture medium composed of alpha minimum essential medium supplemented with 16.5% FBS, 1% (v/v) l-glutamine, and 1% (v/v) penicillin/streptomycin solution was used.

2.4. 3D bioprinting cell-laden cartilage construct

Tabletop stereolithography-based 3D bioprinter was utilized for cell-laden cartilage tissue construct printing. Precursor solutions (GelMA, PEGDA, nanospheres and photoinitiator) were mixed with MSCs at a cell density of 2×10^6 cells ml^{-1}. Cell-laden cartilage constructs were bioprinted as square pattern. To visualize the cell distribution in the bioprinted construct, MSCs were pre-labeled with cell tracker green (Life Technologies). Imaging was conducted by a laser scanning confocal microscope (ZEISS LSM 710). In addition, the printed construct morphology was examined by confocal microscope after staining with blue dye. The positions of nanospheres in the bioprinted construct were also observed. Rhodamine conjugated BSA was encapsulated inside the nanospheres for tracing.

2.5. In vitro growth factor release study

Nanospheres fabricated via electrospraying were incorporated into the hydrogels to improve MSC chondrogenic differentiation. For growth factor release study, BSA as a model protein was encapsulated in nanospheres at concentration of 10 mg ml^{-1} in PBS to evaluate the loading rate and release profile. The growth factor loading rate was determined using an established solvent-extraction technique [20]. In brief, 10 mg of nanospheres were dissolved in dichloromethane for 6 h at 37 °C. PBS solution was then added into the dissolved nanospheres solution for 24 h and the embedded BSA was extracted from organic phase to aqueous phase. The amount of BSA in aqueous phase was determined by Pierce BCA Protein Assay Kit (ThermoFisher).

For the *in vitro* growth release study, the nanospheres were incorporated into the GelMA/PEGDA (10%/5%) solution and printed in to square pattern samples. For comparison, identical BSA was also directly added into the printable bioink and printed in the absence of nanospheres. Each sample was placed in 1 ml of PBS in a microcentrifuge tube and maintained in an incubator at 37 °C for up to 21 d. At each time point, 200 μl of solution was collected for analysis and then fresh PBS was added. Cumulative release of BSA was determined by Pierce BCA protein assay kit over the course of 21 d.

2.6. Cell viability and proliferation studies

GelMA was first dissolved in PBS containing 1% photoinitiator at a concentration of 10%. Precursor solutions were prepared by adding 5%, 10%, 15% and 20% PEGDA into the GelMA/PBS solution. Prior to cell incorporation, the solutions were adjusted by sodium hydroxide to a pH value of 7. Cells encapsulated in hydrogels were cultured up to 5 d. At days 1, 3, and 5, cell proliferation was quantified by cell counting kit-8 (CCK-8, Dojindo Laboratories) assay per manufacturer's instruction. In addition, cell viability in the formulation of GelMA/PEGDA (5%/10%) hydrogel was evaluated after 1 d culture. Live/dead viability assay kit (Life Technologies) was utilized to stain the live and dead cells. The cells were then visualized by confocal microscope.

2.7. Histology analysis

MSCs were encapsulated in bioinks with and without 10 mg ml^{-1} TGF-β1 embedded nanospheres at a density of 5×10^6 cells ml^{-1}. After printing, samples were cultured in chondrogenic differentiation medium composed of complete MSC medium supplemented with 100 nM dexamethasone, 50 μg ml^{-1} L-ascorbic acid, 40 μg ml^{-1} proline, 100 μg ml^{-1} sodium pyruvate, and 1% ITS+. After 3 weeks of incubation, samples were then fixed in 10% formalin for 1 h, embedded in optimum cutting temperature formulation of water-soluble glycols and resins and kept in a freezer. Frozen samples were then sectioned using a freezing microtome to a thickness of 40 μm. The sections were stained with safranin O and alcian blue to bind to cartilage proteoglycan and glycosaminoglycan (GAG). Briefly, safranin O staining was conducted by placing the sections in 0.02% fast green for 3 min followed by incubating with 1% acetic acid for 30 s at room temperature. 0.1% safranin O was then added into the slides for 10 min. After being rinsed with water 3 times, slides were mounted

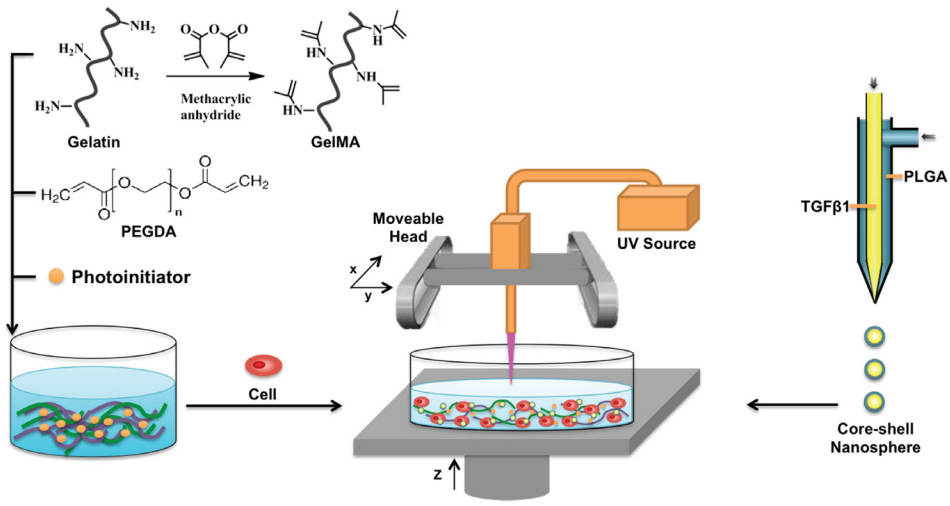

Figure 1. Schematic illustration of bioink preparation and cartialge construct printing.

with coverslip. The alcian staining was performed by immersing slides in mixed 3% alcian blue solution and 3% methanol solution (1:1 v/v). Histological sections were imaged using optical microscopy (Mu800, Amscope) at the same instrument settings.

2.8. Chondrogenic differentiation analysis

Printed constructs with and without nanospheres were cultured in chondrogenic differentiation medium up to 3 weeks. At each time point (week 1, week 2, and week 3), total RNA of each sample was isolated using Trizol reagent (Life Technologies) according to manufacturer's instruction. The concentration of extracted RNA was measured by a NanoDrop1000 spectrophotometer (ThermoScientific). 500 ng RNA was reversely transcribed to complementary DNA (cDNA) using PrimeScript RT reagent Kit (TaKaRa). Quantitative real-time PCR was conducted using Bio-Rad CFX-384 system. A final reaction volume is 20 μl consisting of 10 μl SYBR Premix Ex Taq II (2X), 0.8 μl (10 uM) of each primer, 0.4 μl ROX Reference Dye, 2 μl two-fold diluted cDNA solution, and 6 μl sterile distilled water. Primer sequences: forward 5′-TTCAGCTATGGAGATGACAATC-3′ and reverse 5′-AGAGTCCTAGAGTGACTGAG-3′ for Collagen II a1, forward 5′-GAACGCACATCAAGACGGAG-3′ and reverse 5′-TCTCGTTGATTTCGCTGCTC-3′ for Sox 9, forward 5′-AGCTGGGTTCGGGGCATCT-3′ and reverse 5′-TGGTAGTCTTGGGCATTGTTGTTGA-3′ for Aggrecan, and forward 5′-CCAGGTGGTCTCCTCTGACTTC-3′ and reverse 5′-GTGGTCGTTGAGGGCAATG-3′ for housekeeping gene glyceraldehyde-3-phosphate-dehydrogenase (GAPDH).

2.9. Statistical analysis

The results of all experiments are expressed as mean ± standard deviation and analyzed by student t-test. P value < 0.05 was considered statistical difference.

3. Results

3.1. Preparation and characterization of printable bioink

Figure 1 shows the preparation of bioink and printing of construct. The bioink consists of GelMA, PEGDA and growth factor-loaded nanospheres. The addition of PEGDA into GelMA greatly improved the mechanical properties of resultant hydrogels, presenting proportionally increased compressive modulus with the concentration of PEGDA (figures 2(A), (B)). Pure GelMA hydrogel presented the lowest compressive mechanical property. 5% of PEGDA addition can result in an 8.6-fold increase in compressive modulus. Figure 2(C) summarizes the equilibrium swelling ratio of hydrogels with varying compositions. Generally, the addition of PEGDA decreased the equilibrium swelling ratio which indicates that the hydrogel became more compact. Higher equilibrium swelling ratio is a benefit of cell-laden printing, which offers much more space for cell growth and spreading within the printed construct. There is no apparent change of equilibrium swelling ratio when 5% PEGDA is incorporated into GelMA hydrogel relative to GelMA alone. More than 10% PEGDA addition significantly decreased the equilibrium swelling ratio of GelMA hydrogel ($p < 0.05$). The measurement of line width in figure 2(D) illustrates that the addition of PEGDA into GelMA greatly increased the printing resolution. There is no concentration dependence; the 5% PEGDA addition can achieve as high a printing resolution as does 20% addition.

3.2. Bioprinting of cell-laden construct

As a proof of concept, the construct was printed as a square pattern and morphology was observed by confocal microscope after staining. Figures 3(A), (B) illustrated that the stereolithography-based 3D bioprinter is able to print cartilage construct with well-defined architecture. When nanospheres were encapsulated inside the construct, they were evenly

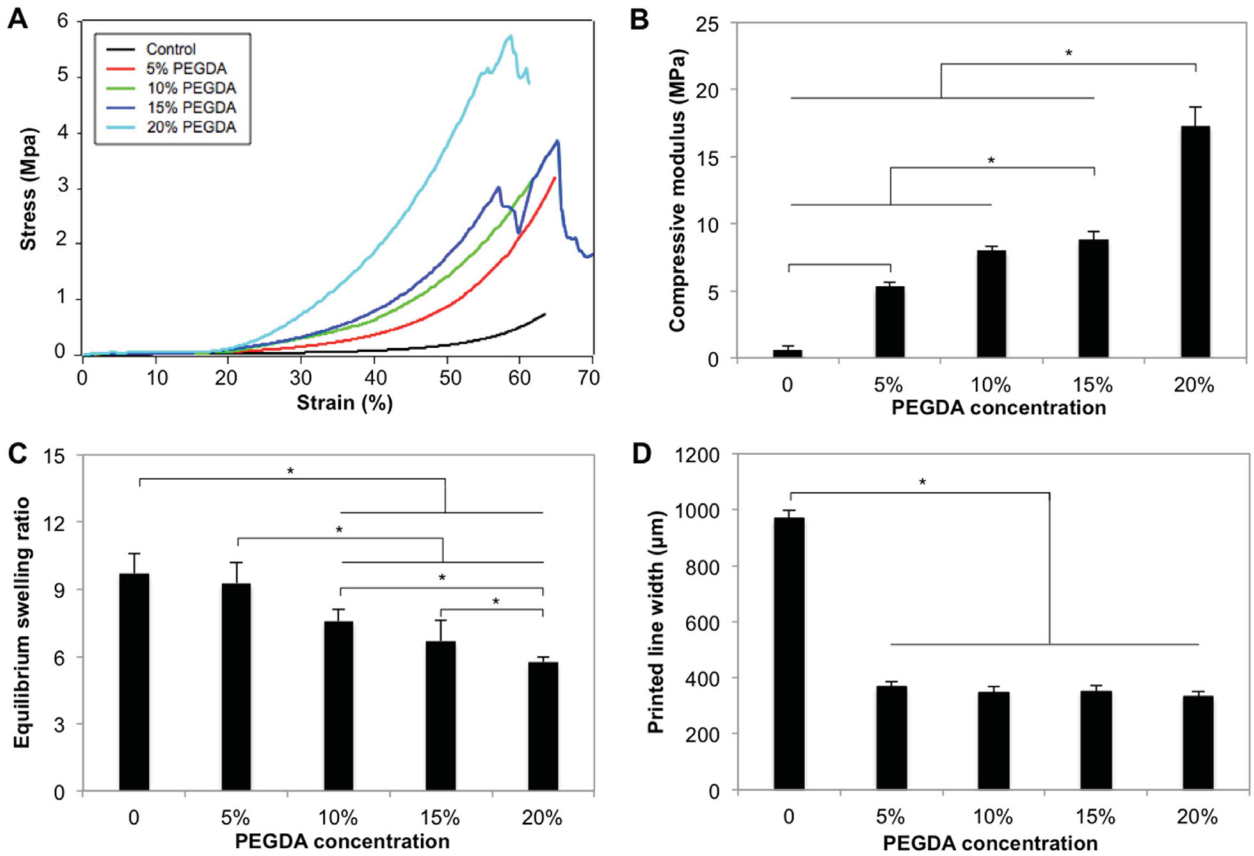

Figure 2. (A) Representative stress–strain curves and (B) compressive moduli of hydrogels with varying PEGDA concentrations. (C) Equilibrium swelling ratio of hydrogels with increasing PEGDA concentrations quantified via wet versus dry samples. (D) Printing resolution change with the PEGDA concentration. $n = 5$, $^{*}p < 0.05$. Data are expressed as mean ± standard deviation.

distributed over the entire construct (figures 3(C), (D)). A homogeneous cell distribution was also observed in the 3D bioprinted construct (figures 3(E), (F)). These results demonstrated the feasibility of our stereolithography-based 3D bioprinting platform for producing cartilage constructs.

3.3. High cell proliferation rate on low concentration hydrogel

The proliferation of MSCs encapsulated in GelMA/PEGDA was evaluated 1, 3, and 5 d (figure 4(A)). The cell proliferation rate was lowest in the case of hydrogel with highest PEGDA addition. This probably resulted from the structure change caused by the additional PEGDA, where the PEGDA made the hydrogel matrix more compact and limited cell proliferation. The equilibrium swelling study also illustrated the lower water retention for the 20% PEGDA-added hydrogel which might lead to insufficient nutrition, oxygen diffusion, and exchange for cell growth.

Figure 4(B) shows the representative images for the live/dead assay of cells encapsulated in GelMA/PEGDA (10%/5%) hydrogel at day 1. Remarkably, MSCs kept viable in 3D bioprinted GelMA/PEGDA construct *in vitro*. Predominant green fluorescence demonstrated the cells maintained high cell viability. The image analysis illustrated that the viability can reach to 75% at day 1. Dead cells were located mainly in the crossing area where the sites were exposed to UV laser twice when the construct was printed.

3.4. Sustained in vitro release of BSA from 3D printed construct with nanospheres

Nanospheres present a spherical shape (figure 5(A)). The release profiles of BSA from 3D bioprinted constructs carrying BSA loaded nanospheres and bare BSA were investigated and results are presented in figure 5(B). There was an initial burst release in the first day; the release of BSA subsequently slowed down and kept a sustained release for more than 21 d. When compared to the BSA loaded in nanospheres, the overall release of bare BSA in 3D bioprinted construct was comparatively fast; a greater initial burst release on the first day was evident. At day 21, there was 33% more BSA release from 3D bioprinted construct with bare BSA when compared to that BSA loaded in nanospheres, indicating the higher retention of growth factors when they are delivered via nanospheres. As the cells are encapsulated inside 3D bioprinted constructs, the higher retention and slow release from constructs will provide longer and more sustained stimulation for cell growth and differentiation inside them.

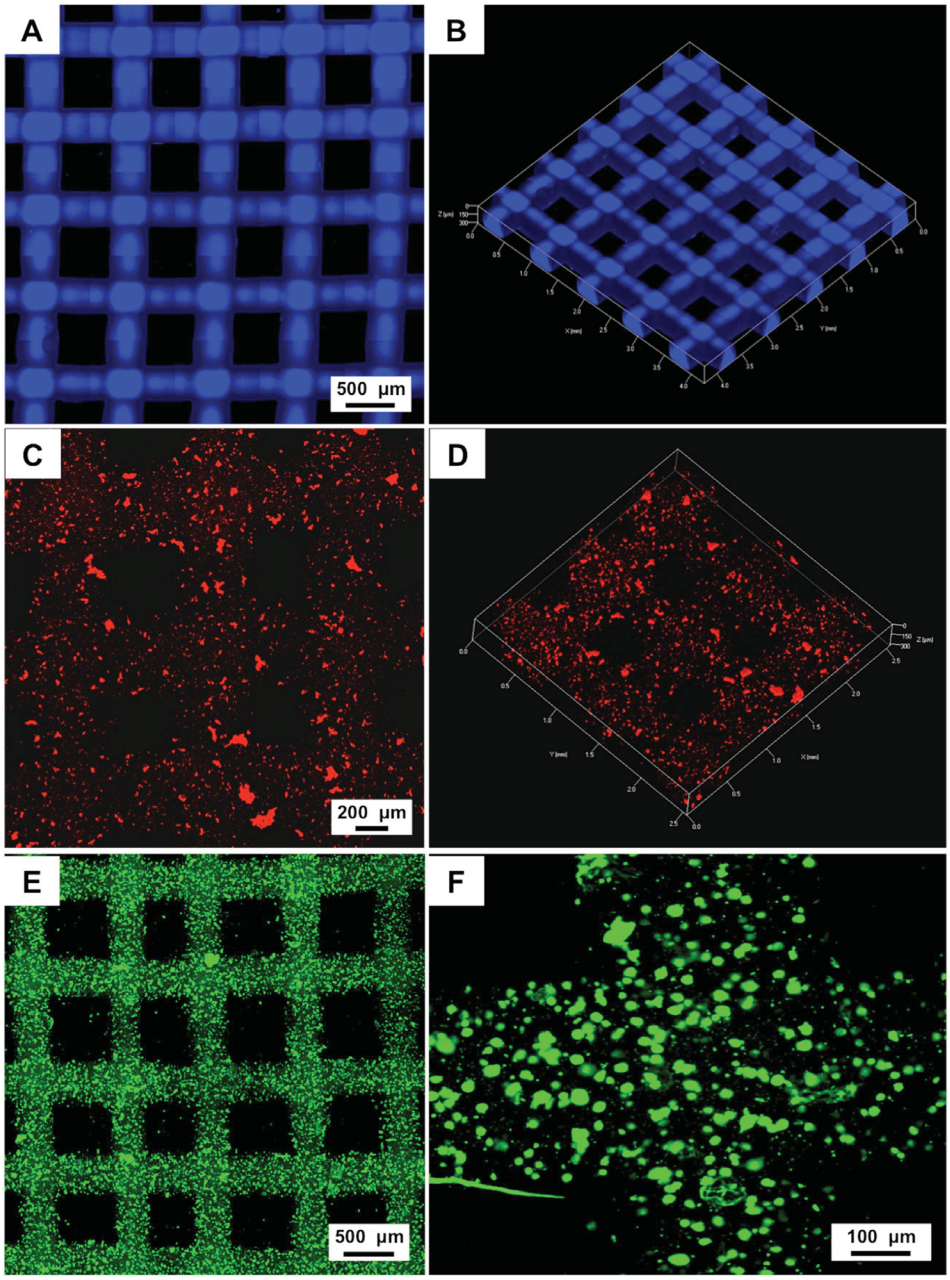

Figure 3. (A) Top and (B) 3D views of bioprinted construct using bioink consisting of 5% PEGDA and 10% GelMA. (C) and (D) indicate the nanospheres distribution in the entire bioprinted construct. (E) and (F) represent the cell distribution in bioprinted construct in low and high magnifications.

3.5. TGF-β1 loaded nanospheres improved chondrogenic differentiation

Bioink for chondrogenic differentiation study was prepared by mixing 10% GelMA base with 5% PEGDA. In addition, TGF-β1-loaded nanospheres were incorporated in the bioink at the concentration of 10 mg ml^{-1}. Bioink without nanospheres was selected as comparison. After 3 weeks of chondrogenic induction, chondrogenic ECM secretions were found on both groups with and without nanospheres (figure 6). To quantify the chondrogenesis of MSCs in two groups, qPCR was performed and the level of chondrogenesis related genes expression was evaluated (figure 7). It was found that MSCs encapsulated in construct loading nanospheres revealed higher expression levels of Collagen II and Aggrecan in the entire period compared to control. The expression of SOX-9 presented higher expression in nanospheres group since week 2. There was a 2.5-fold, 1.6-fold, and 3.4 -fold increase in Collagen II level in TGF-β1 nanospheres containing construct compared with that of bare construct at week 1, week 2, and week 3. The expression level

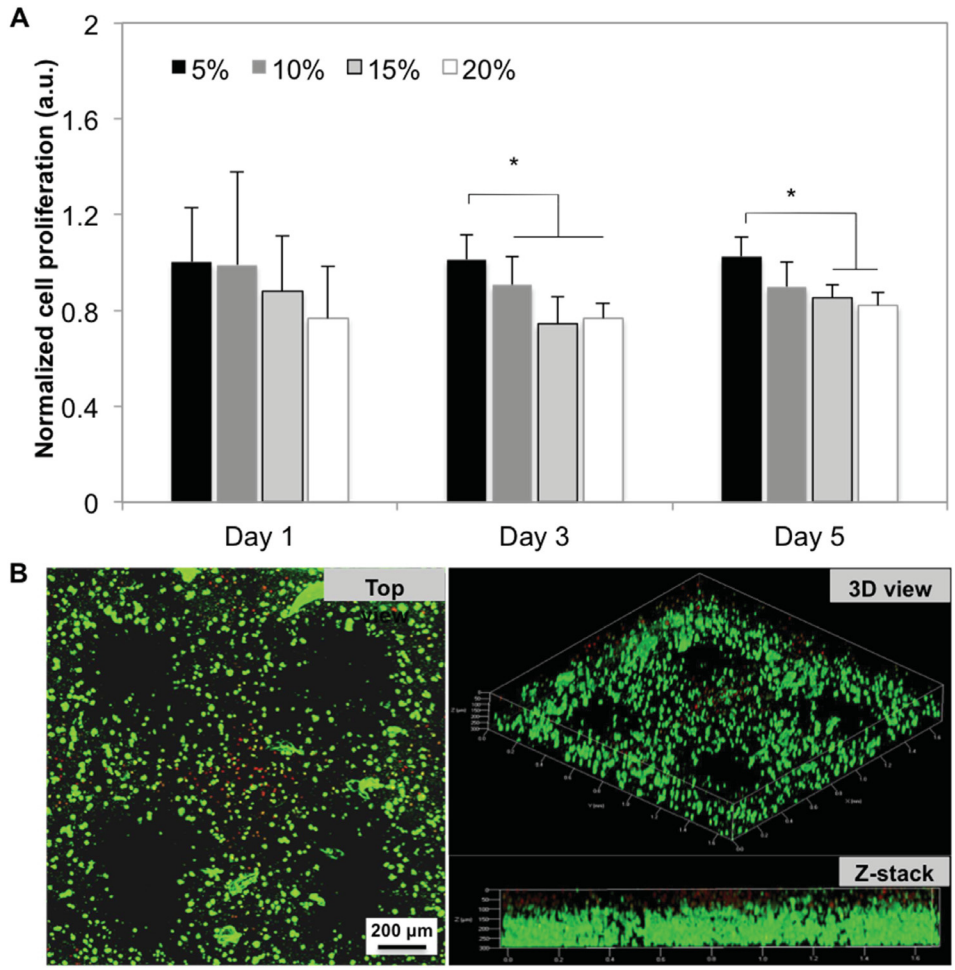

Figure 4. (A) MSCs proliferation when cells were encapsulated in 10% GelMA with varying concentrations of PEGDA hydrogels, $n = 6$, $^{*}p < 0.05$. Data are expressed as mean ± standard deviation. (B) Live-dead cell staining of MSCs within 5% PEGDA/GelMA bioprinted construct after culturing for 1 d. Cells were stained with calcein-AM/ethidium homodimer, and living cells were detected as green fluorescence and dead cells were detected as red fluorescence.

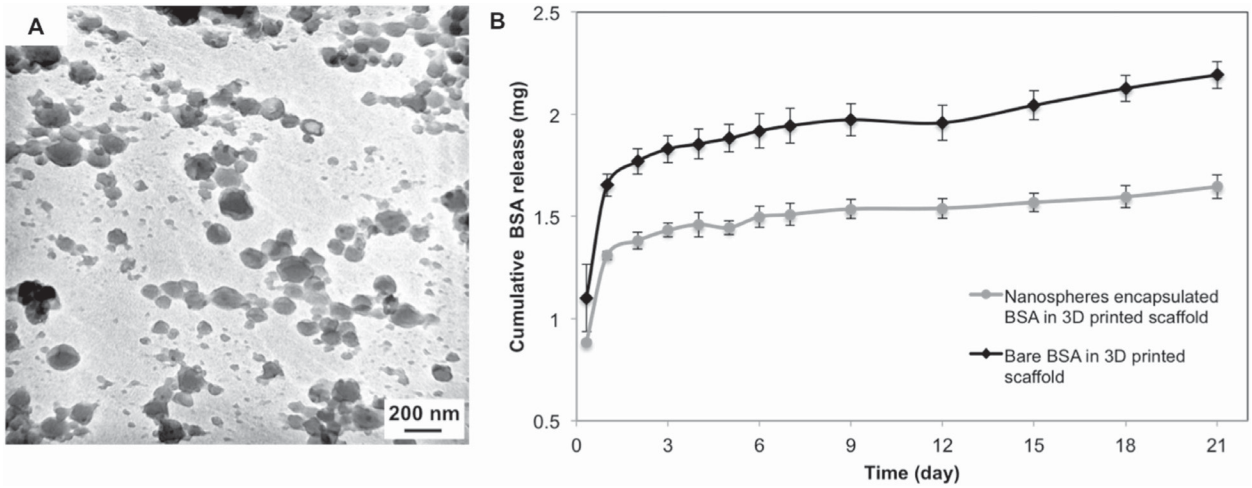

Figure 5. (A) TEM morphology of electrosprayed nanospheres. (B) *In vitro* release profiles of BSA from 3D bioprinted scaffold with BSA loaded nanospheres and bare BSA, $n = 3$. Data are expressed as mean ± standard deviation.

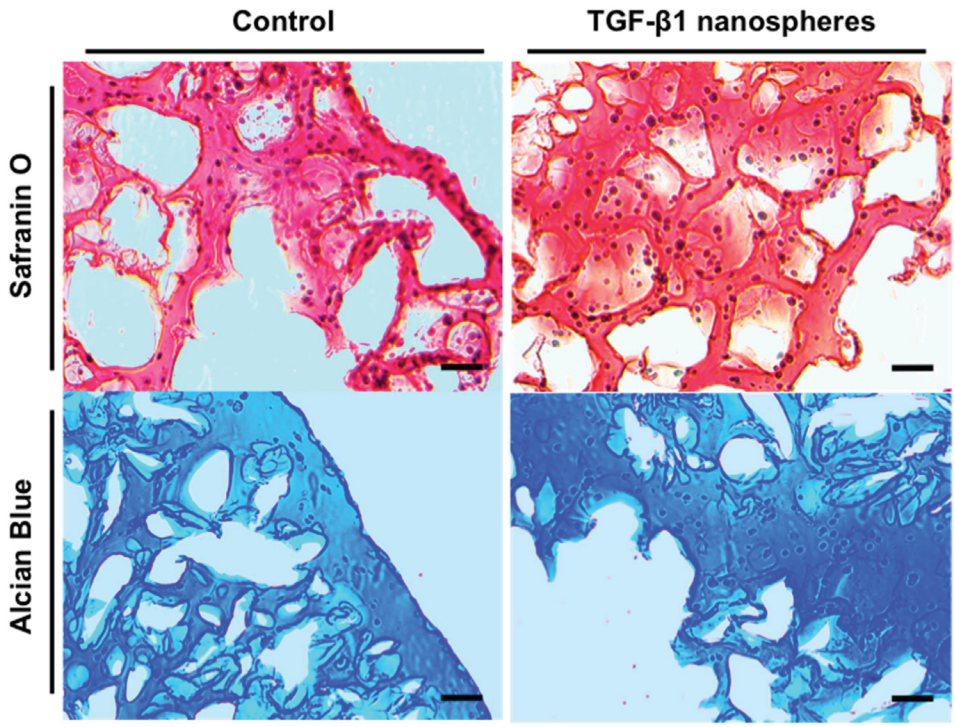

Figure 6. Safranin O and Alcian blue stained histological sections of the hMSCs encapsulated in GelMA/PEGDA hydrogels with and without TGF-β1 containing nanospheres. Samples were cultured in chondrogenic differentiation medium for 3 weeks. Scale bar $= 100\ \mu$m.

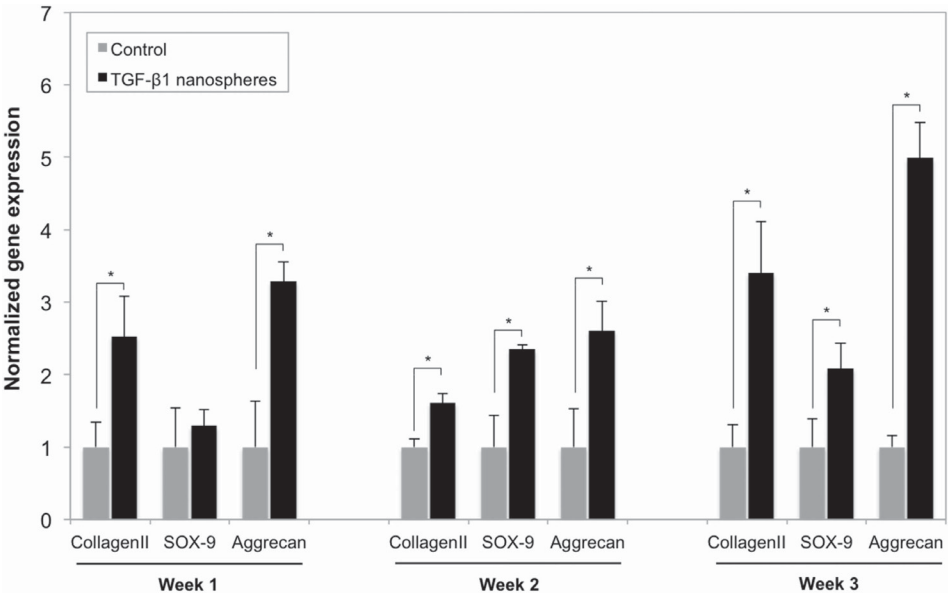

Figure 7. Expression levels of cartilage-specific genes, Collagen II, SOX-9, Aggrecan during 3 weeks chondrogenic differentiation. A significant increase in expression of collagen II and aggrecan on bioprinted constructs with TGF-β1 containing nanospheres over 3 weeks, SOX-9 expression was significantly higher at week 2 and week 3. $n = 3$, $^{*}p < 0.05$. Data are expressed as mean $\pm$ standard deviation.

of Aggrecan kept similar tendency with Collagen II, and there were 3.2-fold, 2.6-fold, and 5.0-fold increases in the group of TGF-β1 nanospheres-containing construct relative to bare construct at three time points, respectively. In the case of SOX-2 expression, there were not significant differences amongst 2 groups at week 1, while 2.3-fold and 2.1-fold up-regulations were observed in TGF-β1 nanospheres containing construct at week 2 and week 3.

4. Discussion

3D printing has been used to create tissue scaffolds with well-defined micro architecture. Some 3D printing techniques permit cell-laden printing (bioprinting) which can significantly enhance the interaction between cells and scaffold matrix for improved tissue regeneration. 3D bioprinting has been explored in scaffold fabrication in multiple tissues, including cartilage, by using different cell types and biomaterials [8, 21]. Hydrogels have been demonstrated to be attractive biomaterials for 3D bioprinting various tissues due to their general biocompatibility, high water retention, and structural similarity to ECM [22, 23]. To be used for bioprinting, the hydrogels must be viscous before bioprinting to permit the inclusion of cells as well as to maintain the structural integrity after solidification by UV photopolymerization, temperature change, or ionic cross-linking post-bioprinting. In the present study, we utilized a stereolithography-based 3D bioprinting technique to fabricate a hydrogel cartilage construct by mixing GelMA and PEGDA. One critical 3D scaffold design criterion is that the scaffold should have suitable mechanical properties mimicking the native tissues. GelMA is a highly biocompatible material with photocrosslinkable capacity that can be used for cell-laden bioprinting. However, undesirable mechanical properties and the printing resolution of GelMA hydrogels compromise their application in 3D bioprinting. Printed scaffolds with GelMA alone tend to collapse. In our study, in order to improve the structural fidelity of printed scaffolds and achieve a leveraged mechanical property, we added PEGDA into GelMA hydrogels, which greatly increased the mechanical property as well as improved printing resolution when compared to GelMA only (figure 2). The printing resolution was significantly increased by adding only 5% PEGDA into GelMA hydrogel. Remarkably, the hydrogel equilibrium swelling ratio was not altered by the incorporation of 5% PEGDA. Swelling ratio is an indicator of hydrogel hydrophilicity, degree of cross-linking, network porosity, and degradation [24]. 5%/10% PEGDA/GelMA hydrogel provides a highly porous structure to allow for cell growth, and migration, as well as nutrition and cell waste exchange, indicating that a more successful tissue regeneration could be achieved.

In addition to the biomaterial selection, the cell type is another crucial feature for successful tissue regeneration using 3D bioprinting approaches. Considering the unique biological properties of stem cells, pilot studies in a variety of systems have demonstrated great prospects for the use of stem cell in tissue engineering [25]. Despite the fact that stem cells have the capacity to differentiate into multiple cell lines, control over the differentiation tendency is difficult. Therefore, when stem cells are used for specific tissue regeneration, bioactive factors, which can promote stem cell differentiation into specific cell lines, are usually required in tissue-engineered scaffolds [12]. Direct addition of bioactive factors into scaffolds might result in their quick release and loss in a short period. To be effective as bioactive agents, growth factors are usually delivered by incorporation into carriers. The carriers can be nanospheres, microspheres, or other similar products that provide more sustained release and prevent denaturing of the bioactive protein factors [26]. In our study, we synthesized core–shell nanospheres to serve as a sustained release system by using electrospraying technique. Coaxial electrospraying is a mature nanosphere fabrication technique and has been widely reported for making core–shell structures. For instance, Cao *et al* found that the technique can create a clear boundary between core and shell regions, demonstrating the formation of a core–shell structure [27]. Our previous study also demonstrated that the electrosprayed nanospheres have a homogeneous size distribution and allow a sustained growth factor release when compared to microspheres [28]. The electrosprayed nanospheres have an average size of 109 nm with diameters ranging between 60 nm and 120 nm [29]. When the nanospheres delivery system is incorporated into the 3D bioprinted cartilage construct, growth factor can be retained inside the construct for a longer time relative to growth factor addition without a carrier (figure 5). Since the cells reside inside the bioprinted construct, a longer retention of growth factor is advantageous for cell growth and new tissue formation.

5. Conclusions

An important challenge for 3D bioprinting is to maintain the viability of living cells and bioactivity of sensitive growth factors and biochemicals. The stereolithography based 3D bioprinting technique developed in our lab has shown the capacity to maintain cell viability and growth factors bioactivity post-printing. Bioprinted cartilage constructs consisting of GelMA and PEGDA show well-defined architecture. When the TGF-β1 encapsulated core–shell nanospheres are included in the bioprinted cartilage construct, chondrogenic differentiation of MSCs was improved significantly. Thus, the 3D bioprinted cartilage construct encapsulating cell and growth factor is a promising strategy for cartilage tissue regeneration.

Acknowledgments

The authors would like to thank the NSF BME program grant #1510561.

ORCID iDs

Wei Zhu https://orcid.org/0000-0003-1809-3578
Lijie Grace Zhang https://orcid.org/0000-0003-3009-045X

References

[1] Huey D J, Hu J C and Athanasiou K A 2012 Unlike bone, cartilage regeneration remains elusive *Science* **338** 917–21
[2] Kolesky D B, Truby R L, Gladman A S, Busbee T A, Homan K A and Lewis J A 2014 3D bioprinting of vascularized, heterogeneous cell-laden tissue constructs *Adv. Mater.* **26** 3124–30

[3] Holmes B, Zhu W, Li J, Lee J D and Zhang L G 2015 Development of novel three-dimensional printed scaffolds for osteochondral regeneration *Tissue Eng.* A **21** 43–415
[4] Hollister S J 2005 Porous scaffold design for tissue engineering *Nat. Mater.* **4** 518–24
[5] Murphy S V and Atala A 2014 3D bioprinting of tissues and organs *Nat. Biotechnol.* **32** 773–85
[6] Falconnet D, Csucs G, Michelle Grandin H and Textor M 2006 Surface engineering approaches to micropattern surfaces for cell-based assays *Biomaterials* **27** 3044–63
[7] Zhou X *et al* 2016 3D bioprinting a cell-laden bone matrix for breast cancer metastasis study *ACS Appl. Mater. Interfaces* **8** 30017–26
[8] Markstedt K *et al* 2015 3D bioprinting human chondrocytes with nanocellulose-alginate bioink for cartilage tissue engineering applications *Biomacromolecules* **16** 1489–96
[9] Guillotin B *et al* 2010 Laser assisted bioprinting of engineered tissue with high cell density and microscale organization *Biomaterials* **31** 7250–6
[10] Iwami K, Noda T, Ishida K, Morishima K, Nakamura M and Umeda N 2010 Bio rapid prototyping by extruding/aspirating/refilling thermoreversible hydrogel *Biofabrication* **2** 014108
[11] Xu T, Jin J, Gregory C, Hickman J J and Boland T 2005 Inkjet printing of viable mammalian cells *Biomaterials* **26** 93–9
[12] Chen F-M, Zhang M and Wu Z-F 2010 Toward delivery of multiple growth factors in tissue engineering *Biomaterials* **31** 6279–308
[13] Park T G, Jeong J H and Kim S W 2006 Current status of polymeric gene delivery systems *Adv. Drug Deliv. Rev.* **58** 467–86
[14] Qiu L Y and Bae Y H 2006 Polymer architecture and drug delivery *Pharm. Res.* **23** 1–30
[15] Danhier F, Ansorena E, Silva J M, Coco R, Le Breton A and Préat V 2012 PLGA-based nanoparticles: an overview of biomedical applications *J. Control. Release* **161** 505–22
[16] Golub J S *et al* 2010 Sustained VEGF delivery via PLGA nanoparticles promotes vascular growth *Am. J. Physiol. Heart. Circ. Physiol.* **298** H1959–65
[17] Van Den Bulcke A I, Bogdanov B, De Rooze N, Schacht E H, Cornelissen M and Berghmans H 2000 Structural and rheological properties of methacrylamide modified gelatin hydrogels *Biomacromolecules* **1** 31–8
[18] Nichol J W, Koshy S T, Bae H, Hwang C M, Yamanlar S and Khademhosseini A 2010 Cell-laden microengineered gelatin methacrylate hydrogels *Biomaterials* **31** 5536–44
[19] Zhu W, Masood F, O'Brien J and Zhang L G 2015 Highly aligned nanocomposite scaffolds by electrospinning and electrospraying for neural tissue regeneration *Nanomed.: Nanotechnol. Biol. Med.* **11** 693–704
[20] Lu L, Stamatas G N and Mikos A G 2000 Controlled release of transforming growth factor beta 1 from biodegradable polymer microparticles *J. Biomed. Mater. Res.* **50** 440–51
[21] Weigelt B and Bissell M J 2008 Unraveling the microenvironmental influences on the normal mammary gland and breast cancer *Sem. Cancer Biol.* **18** 311–21
[22] Cui H T, Nowicki M, Fisher J P and Zhang L G 2017 3D bioprinting for organ regeneration *Adv. Healthc. Mater.* **6** 1601118
[23] Stanton M M, Samitier J and Sánchez S 2015 Bioprinting of 3D hydrogels *Lab Chip* **15** 3111–5
[24] Zustiak S P and Leach J B 2010 Hydrolytically degradable poly(ethylene glycol) hydrogel scaffolds with tunable degradation and mechanical properties *Biomacromolecules* **11** 1348–57
[25] Bianco P and Robey P G 2001 Stem cells in tissue engineering *Nature* **414** 118–21
[26] Panyam J and Labhasetwar V 2003 Biodegradable nanoparticles for drug and gene delivery to cells and tissue *Adv. Drug Deliv. Rev.* **55** 329–47
[27] Cao Y, Wang B, Wang Y and Lou D 2014 Polymer-controlled core–shell nanoparticles: a novel strategy for sequential drug release *RSC Adv.* **4** 30430–9
[28] Zhu W, Masood F, O'Brien J and Zhang L G 2015 Highly aligned nanocomposite scaffolds by electrospinning and electrospraying for neural tissue regeneration *Nanomed.: Nanotechnol. Biol. Med.* **11** 693–704
[29] Zhu W, Lee S J, Castro N J, Yan D, Keidar M and Zhang L G 2016 Synergistic effect of cold atmospheric plasma and drug loaded core–shell nanoparticles on inhibiting breast cancer cell growth *Sci. Rep.* **6** 21974